

Weak anisotropy of the in-plane magnetoresistance in high mobility (100) Si-MOS structures

V. M. Pudalov^a, G. Brunthaler^b, A. Prinz^b, G. Bauer^b

^a *P. N. Lebedev Physics Institute, 117924 Moscow, Russia.*

^b *Institut für Halbleiterphysik, Johannes Kepler Universität, Linz, Austria*
(May 15, 2019)

This letter reports studies of the magnetoresistance in two-dimensional electron system in (100) Si-MOSFETs, for perpendicular and parallel orientations of the current with respect to the magnetic field in the 2D-plane. Although the magnetoresistance is almost isotropic, in the hopping regime it contains a weak non-monotonic anisotropic component. The results support a spin- but not orbital origin of the parallel field magnetoresistance in Si-MOSFETs. The data enabled us to estimate the renormalization of the Zeeman splitting for r_s up to $\approx 9 - 11$. The results are found to be *inconsistent with a simple picture of the spin polarization of free 2D electrons* and are discussed in terms of the spin polarization of localized states.

PACS: 71.30.+h, 73.40.Hm, 73.40.Qv

For low carrier densities, in the vicinity of the phenomenon known as ‘metal-insulator transition (MIT) in two dimensions’, a magnetic field B_{\parallel} applied in the plane of the 2D carriers suppresses the anomalous metallic conduction [1–5]. The observed strong magnetoresistance (MR) and subsequent saturation of the resistivity in high fields is often interpreted as a manifestation of the spin alignment of free carriers by parallel field [4]. Recently, in Ref. [6], the strong MR was suggested to be an orbital effect caused by the transition from 2D to 3D behavior, when the magnetic length a_B becomes smaller than the thickness of the quasi-2D layer. We note however, that there is another possibility in which the parallel field also acts on the spins of the localized carriers (or of the donor/acceptor bound states), and causes a corresponding increase in Coulomb scattering. Such a possibility is particularly inherent in the models [7,8] relying on interface trap states.

In order to determine the relevance of spin effects, we have performed measurements of the MR for a magnetic field in the 2D plane, with bias current j perpendicular and parallel to the field. In the explored range of densities close to and through the MIT, and in magnetic fields ($0 \div 12$) T, we found *no strong anisotropy* as predicted in Ref. [6]. This suggests the spin but not orbital origin of the MR in Si-MOS structures. We revealed only a weak anisotropy in the MR, $\Delta\rho = (\rho_{\parallel} - \rho_{\perp})/2\bar{\rho} \sim 5\%$, which in the hopping regime exhibits a peak-shape structure as a function of the magnetic field. To the best of our knowledge, such an asymmetry in the (100) crystal plane has not been observed earlier in 2D systems (a monotonic anisotropy of the MR was reported recently in Ref. [9] for the anisotropic GaAs/AlGaAs (311) plane but this seems irrelevant to our case). The anisotropic component of the MR indicates the contribution of zero-field spin-orbit (SO) coupling to the hopping transport in the vicinity of the MIT.

The ac-measurements (3 Hz) of the resistivity were performed at temperatures 0.27 – 0.3 K on three (100) Si-MOS samples: Si-9Nj (peak mobility $\mu^{peak} = 4.14 \text{ m}^2/\text{Vs}$ at $T = 0.3 \text{ K}$), Si-153 ($3.8 \text{ m}^2/\text{Vs}$), and Si-43 ($1.96 \text{ m}^2/\text{Vs}$). The samples were lithographically defined as rectangular Hall bars of the size $0.8 \times 5 \text{ mm}$ (Si-9Nj and Si-153) and $0.256 \times 2.5 \text{ mm}$ (Si-43); their long sides (current direction) were aligned along [010]. We present mainly data for one sample (Si-9Nj) studied in most detail; two other samples exhibited qualitatively similar behavior of $R(B_{\parallel})$. Typical field dependent traces of the resistivity are shown in Fig. 1. Similar to that reported earlier [1,2], resistivity grows with magnetic field and then saturates above a certain field, B_{sat} . To obtain the data for different orientations of j relative to B_{sat} , the sample was rotated *in situ* at low temperature.

Figure 1 demonstrates (i) the absence of a large anisotropy in the MR, and (ii) the presence of a minor anisotropy (within 12%) in high fields and for intermediate densities with $\rho(j \parallel B)$ systematically exceeding $\rho(j \perp B)$ [10]. Both these results disagree with the predictions of Ref. [6] where the MR was associated with a crossover from 2D to 3D behavior with increasing parallel field. A weak non-monotonic difference (2-5%) between $\rho(j \parallel B)$ and $\rho(j \perp B)$ in lower fields will be discussed further. In order to quantify the saturation field B_{sat} , we used two different empiric definitions for B_{sat} as a field corresponding to: (1) interception of the tangents (as demonstrated in Fig. 1); (2) increase of the MR to 97.5% of its maximum value. The two dashed lines in Fig. 1 connect the $\rho(B_{\text{sat}})$ -points determined according to the definitions (1) and (2).

The measured $B_{\text{sat}}^{\text{exp}}$ -data are plotted in Fig. 2 vs electron density. Consistent with earlier results [2,4,5], we find $B_{\text{sat}}^{\text{exp}}$ to be approximately proportional to the density and therefore assume first that the saturation field corresponds to complete polarization of the 2D electron

system,

$$B_{\text{sat}} = \frac{2E_F}{g^* \mu_B}, \quad (1)$$

where g^* is the Landé g -factor and μ_B is the Bohr magneton. E_F and g^* depend only on the carrier density, and B_{sat} should thus be a universal function of the density n . Contrary to this expectation, we found $B_{\text{sat}}^{\text{exp}}(n)$ (for both definitions) to be noticeably different for various samples (see Fig. 2). It follows therefore that the magnetic field value at which the magnetoresistance saturates *does not reflect the spin alignment of the free carriers*. This result, evidently, disagrees with a recently proposed mode [11] where the MR is related solely to the screening radius (or to the density of states at E_F). We assume that the measured $B_{\text{sat}}^{\text{exp}}$ -values include a disorder-dependent additive offset in addition to that described by Eq. (1) $B_{\text{sat}}^{\text{exp}} = B_{\text{sat}}(n) - B_0(\text{disorder})$.

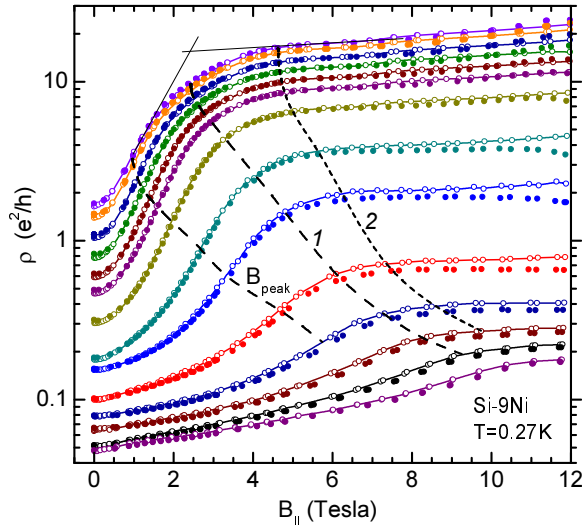


FIG. 1. Resistivity vs in-plane magnetic field. Open symbols are for $j \parallel B$, closed symbols for $j \perp B$. Densities n in units of 10^{11} cm^{-2} are (from top to bottom): 0.748, 0.759, 0.78, 0.80, 0.835, 0.858, 0.913, 1.023, 1.133, 1.353, 1.573, 1.793, 2.013 , $2.233 \times 10^{11} \text{ cm}^{-2}$. Dashed curves 1, 2 correspond to two definitions of the “saturation field” as described in the text, curve B_{peak} depicts the position of the anisotropy peak. Two tangents at the most top curve illustrate definition 1 of B_{sat} .

For high densities, $B_{\text{sat}}^{\text{exp}}(n)$ -data follow a linear dependence whose slope is about twice smaller than the single-particle value [12], $dB_{\text{sat}}/dn = 2\pi\hbar^2/(g_v g_0 m_0 \mu_B) = 10.88$ (where B is in Tesla, n is in 10^{11} cm^{-2} , valley degeneracy $g_v = 2$, and $g_0 = 2$, $m_0 = 0.19$ are the corresponding bare band values). Since the experiment is performed for rather large values of the interaction parameter $r_s = 5.5 - 11$, we consider the Fermi-liquid (FL) renormalization of the two relevant quantities, g -factor g^* and the effective mass $m^* = 2\sqrt{2} \frac{\partial \epsilon}{\partial k} |_{k_F} / r_s^2$:

$$g^*/g_0 = (1 + F_0^a)^{-1} \quad m^*/m_0 = 1 + \frac{1}{2} F_1^s. \quad (2)$$

Here r_s is the ratio of the Coulomb- to Fermi energy, F_0^a and F_1^s are dimensionless spin-antisymmetric (symmetric) interaction functions [13–16].

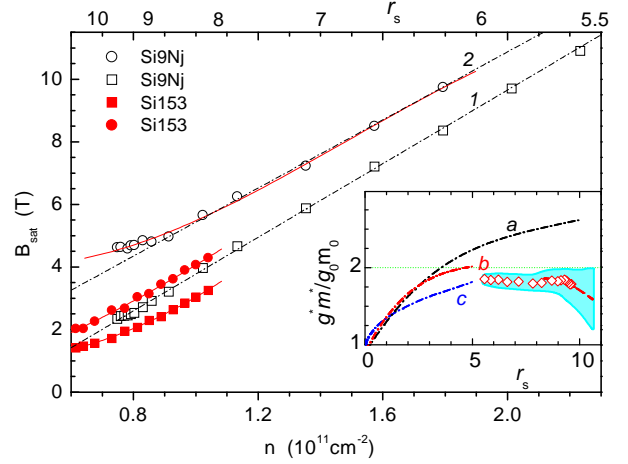


FIG. 2. $B_{\text{sat}}^{\text{exp}}$ vs electron density for two samples. Upper axes shows major r_s values. Circles and squares correspond to two definitions of the “saturation field”. Open symbols are for Si9Nj, closed ones for Si153. Dash-dotted lines are the linear fits, (1) $B_{\text{sat}}^{\text{exp}} = 5.84(n - 0.36)$, (2) $B_{\text{sat}}^{\text{exp}} = 5.44n$ where B is in Tesla and n in 10^{11} cm^{-2} . Inset shows calculated g^*m^*/g_0m_0 vs r_s with g^* from Ref. [13] (curve a), [14] (b), and [15] (curve c); for all curves we used m^* from Eq. (4). g^*m^* -values obtained from $B_{\text{sat}}^{\text{exp}}$ are shown by diamonds (Si9Nj) and dashed curve (Si153) with a shadowed error corridor.

We rewrite the saturation field in terms of the renormalized parameters:

$$B_{\text{sat}} = \frac{\pi\hbar^2 n}{g^* m^* \mu_B} = \frac{\pi\hbar^2 n}{g_0 m_0 \mu_B} \frac{(1 + F_0^a)}{(1 + \frac{1}{2} F_1^s)}. \quad (3)$$

From both, analytical [16] and numerical [14] calculations, the renormalization in g^* (numerator) should be much stronger than in m^* (denominator). The latter one obtained for $r_s \leq 5$ from variational numerical calculations [14], is a slowly varying function of r_s . We fitted the calculated $m^*(r_s)$ with a second order polynomial [17]:

$$m^*/m_0 = 0.9052 + 0.0209r_s + 0.00205r_s^2. \quad (4)$$

Extrapolation to larger r_s values gives a rough estimate for the variation of m^*/m_0 through the entire range of our measurements: from 1.06 at $r_s = 5$ (the upper boundary of calculations) to 1.35 at $r_s = 10.5$. In the inset to Fig. 2, the dashed lines (a, b, c) represent g^*m^* values calculated by using m^* from Eq. (4) and g^* from Refs. [13–15].

Since the offset, $B_0(\text{disorder})$, is sample (and disorder) dependent, we eliminate it for each data set. In order to do this, we note that in the density range

$(0.9 - 2.2) \times 10^{11} \text{cm}^{-2}$, the $B_{\text{sat}}^{\text{exp}}(n)$ -data are well fitted with a linear function the slope of which may be interpreted in accord with Eq. (3) whereas the offset we demand to be zero. It appears that better agreement between all samples is obtained for the definition (1). The values of $g^*m^* = \pi \hbar^2 \mu_B^{-1} (n/B_{\text{sat}})$ obtained in this way are shown by diamonds in the inset to Fig. 2; they agree with calculated ones for $r_s < 9$ but seem to decrease for higher r_s . The same g^*m^* values for $r_s < 8$ could be directly obtained from the slope $(dB_{\text{sat}}/dn)^{-1}$.

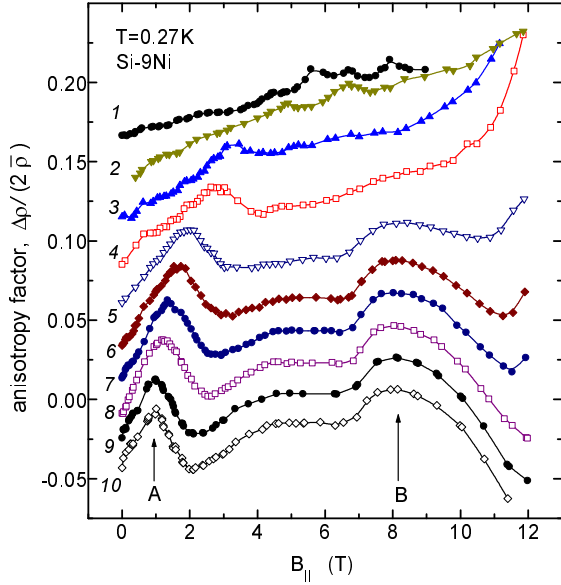


FIG. 3. Anisotropy of the MR vs parallel field. For clarity, the curves are offset shifted vertically by 0.02 relative to each other. Arrows ‘A’ and ‘B’ show two major features. The densities n in units of 10^{11}cm^{-2} are (from bottom to top): 0.748, 0.759, 0.78, 0.80, 0.835, 0.858, 0.913, 1.023, 1.133, 1.353.

Neither the calculated g^* , nor m^* exhibit a decrease with r_s . Almost the whole explored region of $B_{\text{sat}}^{\text{exp}}(n)$ corresponds to the hopping conduction and, therefore, the decrease in g^*m^* for $r_s \geq 9.5$ is not related to the critical density for the MIT. The decrease of g^*m^* is the consequence of the ‘saturation’ in the $B_{\text{sat}}^{\text{exp}}(n)$ dependence (seen in Fig. 2). The $B_{\text{sat}}^{\text{exp}}(n)$ -data in the range $r_s > 9.5$ are, however, partly sample-dependent and the expanding error corridor reflects this uncertainty. The ‘saturation’ in the $B_{\text{sat}}^{\text{exp}}(n)$ and its non-universality may reflect the departure of the above model and be related to the pinning of the Fermi energy at an ‘external’ small band of localized states such as an impurity- or lower Hubbard band. The existence of a band of localized states is consistent with weak changes in the mobile carrier density, as observed in Ref. [18] in the vicinity of the MIT. Finally, the MR saturation may be related to the Zeeman energy in the ‘external’ band of bound states and $\rho(B_{\parallel})$ may reflect its energy profile.

More detailed analysis of the $\rho(B_{\parallel})$ reveals a weak

non-monotonic difference between MR measured with different current polarization, $\Delta\rho = \rho(j \parallel B) - \rho(j \perp B)$ (see Fig. 3). Arrows mark two major features, a density dependent peak ‘A’ and a density independent broad maximum ‘B’. Both peaks are well pronounced only in the hopping regime and disappear for densities $n \gtrsim 1 \times 10^{11} \text{cm}^{-2}$. Whereas the monotonic component of the MR anisotropy (Fig. 3) might in principle be somehow related to the effects of finite thickness of the 2D layer [6], it is not the case for the peak- structure of the MR. We also note that both peaks can not be caused by a perpendicular field component due to a minor misalignment (by $\sim 2^\circ$) [19].

Figure 4 shows that (i) the magnetic field position B_{peak} of the peak ‘A’ increases linearly with density, and (ii) the peak is pronounced only in the hopping regime (i.e., for $\rho(B, n) \gtrsim (0.2 - 2)h/e^2$, depending on the magnetic field). The above two features suggest that the peak may be a manifestation of the zero-field SO coupling in the hopping conduction. Indeed, a peak of a similar shape in the MR anisotropy was predicted in Ref. [20] to occur, due to the interplay between the SO and Zeeman coupling, at such field where

$$g^* \mu_B B_{\text{peak}} = 2\alpha/\xi. \quad (5)$$

Here α is the SO coupling constant, and ξ is the localization length.

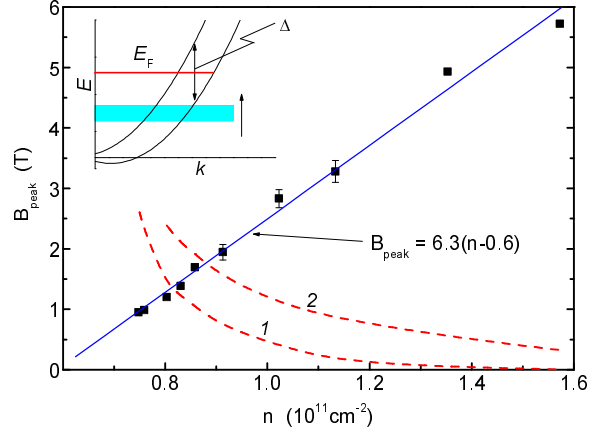


FIG. 4. Magnetic field position of the peak ‘A’ vs electron density. Solid line is a linear fit of the data, dashed curves 1, 2 represent calculated B_{peak} -value from Eq. (5) with two estimates for ξ in the 2D bulk. Inset shows schematically the energy spectrum for free electrons (at $B \neq 0$) and the band of localized states (shaded). The arrow up shows its shift with in-plane magnetic field. Vertical arrow around E_F indicates the ‘energy gap’ Δ combined of SO and Zeeman splitting [15].

To compare with this theoretical picture, we take $\alpha = 6 \times 10^{-6} \text{K cm}$ [21] measured from beating period of the Shubnikov-de Haas oscillations (though for higher n). We assume first the interplay develops solely in the 2D

system and use two estimates for the localization length: (1) $\xi = l$, and (2) $\xi = l \exp(k_F l)$, where l is the mean free path. As shown in Fig. 4, both calculated $B_{\text{peak}}(n)$ -curves have nothing in common with the measured one.

The above inconsistencies indicate that the anisotropy of the MR (and, possibly, the strong MR itself) is related mainly to the spin polarization and SO coupling in an ‘external’ band of localized states rather than in the 2D carrier system. In this modified picture, the MR in parallel field is caused by lifting of the ‘external’ acceptor band (shown schematically in Fig. 4), its depopulation and subsequent increase in the Coulomb scattering rate. The hopping conduction takes place in (or via) the ‘external’ band and the peak in the MR anisotropy should be related to the localization length in the same band. Therefore, ξ may be expected to diverge as $(n - n_c)^{-1}$ which results in the density dependence

$$B_{\text{peak}} \propto 2\alpha(n - n_c)/g^* \mu_B. \quad (6)$$

The solid line in Fig. 4 depicts the best fit to the data, $B_{\text{peak}} = 6.3 \times (n - 0.6)$, where B_{peak} is in T and n is in 10^{11}cm^{-2} . The offset in the fitted dependence agrees with the critical density $n_c = 0.7 \times 10^{11} \text{cm}^{-2}$ within the uncertainty of its determination [22] from $d\rho/dT$ at $B = 0$, the slope agrees with $2\alpha/g^* m^* = 6.49 \pm 0.35$, and the peak in the anisotropy is thus consistent with the above assumption on the hopping conduction in the localized band.

In conclusion, we have shown that the parallel-field magnetoresistance in (100) Si-MOSFETs is almost independent of the relative orientation of the bias current and magnetic field. This is inconsistent with the orbital origin of the strong MR and supports its spin-origin. Within the assumption that the saturation in the MR is associated with complete spin-alignment of a certain band of carriers, the Zeeman splitting for this band is found to be enhanced by 1.85 ± 0.1 times (as compared with the bare band value) in the range of $r_s = 5.5 - 9.5$, in agreement with the numerical calculations. For $r_s > 9.5$, the $B_{\text{sat}}^{\text{exp}}$ tends to saturate as the density decreases, but the interpretation of the data is less clear. We have revealed an intriguing weak ($\approx 4\%$) non-monotonic anisotropy of the MR in the hopping regime, with a density dependent sharp peak and a broad maximum. We relate the sharp peak to the interplay between the SO- and Zeeman coupling in the hopping conduction and find the peak shape and the magnetic field position to be qualitatively consistent with Ref. [20]. The results obtained indicate that (i) the weak anisotropy of the MR and the MR itself may be related mainly to the polarization of spins of bound states rather than of the 2D carriers, and (ii) a narrow acceptor band of localized states is present near the Fermi energy at high r_s values.

The work was supported by FWF (project No 13439), INTAS, RFBR, NATO, Programs ‘Physics of solid state nanostructures’, ‘Statistical physics’ and ‘Integration’.

-
- [1] D. Simonian, S. V. Kravchenko, M. P. Sarachik, V. M. Pudalov, Phys. Rev. Lett. **79**, 2304 (1997).
 - [2] V. M. Pudalov, G. Brunthaler, A. Prinz, G. Bauer, JETP Lett. **65**, 932 (1997). Physica B **249-251**, 697 (1998).
 - [3] M. Y. Simmons, A. R. Hamilton, M. Pepper, E. H. Linfield, P. Rose, D. A. Ritchie, A. K. Savchenko, T. G. Griffiths, Phys. Rev. Lett. **80**, 1292 (1998).
 - [4] T. Okamoto, K. Hosoya, S. Kawaji, A. Yagi, Phys. Rev. Lett. **82**, 3875 (1999). cond-mat/9906425.
 - [5] J. Yoon, C. C. Li, D. Shahar, D. C. Tsui, M. Shayegan, cond-mat/9907128.
 - [6] S. Das Sarma, E. H. Hwang, cond-mat/9909452.
 - [7] B. L. Altshuler, D. L. Maslov, Phys. Rev. Lett. **83**, 2092 (1999).
 - [8] T. M. Klapwijk, S. Das Sarma, Sol. St. Commun. **110**, 581 (1999).
 - [9] S. J. Papadakis, E. P. De Poortere, M. Shayegan, cond-mat/9911239.
 - [10] A minor difference in ρ taken with $j_{\perp} B$ and $j_{\parallel} B$ can be also seen at $B = 0$. This indicates a minor difference in the free carrier density, $\sim 2.5 \times 10^8 \text{cm}^{-2}$ in these two measurement runs.
 - [11] V. T. Dolgoplov, A. Gold, JETP Lett., **71**, 42 (2000).
 - [12] In Ref. [2], the reported value for g^* should be multiplied by a factor of 2.
 - [13] N. Iwamoto, Phys. Rev. B **43**, 2174 (1991).
 - [14] Y. Kwon, D. M. Ceperley, R. M. Martin, Phys. Rev. B **50**, 1684 (1994).
 - [15] G.-H. Chen, M. E. Raikh, Phys. Rev. B **60**, 4826 (1999).
 - [16] A. M. Finkelstein, in: Sov. Sci. Rev. A: Phys. **14**, 1 (1990).
 - [17] The cyclotron mass measured from the amplitude of Shubnikov-de Haas effect (e.g. by W. Pan, D. C. Tsui and B. L. Draper, Phys. Rev. B **59**, 10208 (1999)) is affected mainly by orbital effects (inter-Landau-level exchange) and is irrelevant here.
 - [18] V. M. Pudalov, G. Brunthaler, A. Prinz, and G. Bauer, JETP Lett. **70**, 48 (1999). [Pis'ma ZhETF **70**, 48 (1999)].
 - [19] A perpendicular field component due to its possible misalignment by the angle θ , $B_{\perp} = \sin(\theta) B_{\text{total}}$, in the vicinity of the MIT should induce the re-entrant insulating state with peaks in ρ_{xx} at filling factors $\nu = 1.5$ and $2.5 - 3$. The peaks should thus be located at $B_{\text{total}} = n/[0.2418\nu \sin(\theta)]$, where B is in T and n is in 10^{11}cm^{-2} . The magnetic field for the observed peak ‘B’ is however density independent, whereas the dB_{peak}/dn for the peak ‘A’ is about $10\times$ smaller than the above estimate.
 - [20] G.-H. Chen, M. E. Raikh, and Y.-S. Wu, cond-mat/9904451.
 - [21] V. M. Pudalov, G. Brunthaler, A. Prinz, and G. Bauer, E. M. Dizhur, to be published. The value for α reported earlier (by V. Pudalov, JETP Lett., **66**, 175 (1997)) is overestimated by a factor of three.
 - [22] B. L. Altshuler, D. L. Maslov, V. M. Pudalov, cond-mat/0003032.